NeuroImage 125 (2016) 515–521

Contents lists available at ScienceDirect

NeuroImage

journal homepage: www.elsevier.com/locate/ynimg

Three-dimensional localization of cortical electrodes in deep brain stimulation surgery from intraoperative fluoroscopy

Michael J. Randazzo [a,1], Efstathios D. Kondylis [a,1], Ahmad Alhourani [a], Thomas A. Wozny [a], Witold J. Lipski [a], Donald J. Crammond [a], R. Mark Richardson [a,b,c,*]

[a] Brain Modulation Laboratory, Department of Neurological Surgery, University of Pittsburgh Medical Center, Pittsburgh, PA, USA
[b] Department of Neurobiology, University of Pittsburgh School of Medicine, Pittsburgh, PA, USA
[c] Center for the Neural Basis of Cognition, University of Pittsburgh School of Medicine, Pittsburgh, PA, USA

ARTICLE INFO

Article history:
Received 10 August 2015
Accepted 25 October 2015
Available online 28 October 2015

Keywords:
Deep brain stimulation (DBS) surgery
Electrocorticography (ECoG)
Electrode localization
Fluoroscopy
Image coregistration
Movement disorders

ABSTRACT

Electrophysiological recordings from subdural electrocorticography (ECoG) electrodes implanted temporarily during deep brain stimulation (DBS) surgeries offer a unique opportunity to record cortical activity for research purposes. The optimal utilization of this important research method relies on accurate and robust localization of ECoG electrodes, and intraoperative fluoroscopy is often the only imaging modality available to visualize electrode locations. However, the localization of a three-dimensional electrode position using a two-dimensional fluoroscopic image is problematic due to the lost dimension orthogonal to the fluoroscopic image, a parallax distortion implicit to fluoroscopy, and variability of visible skull contour among fluoroscopic images. Here, we present a method to project electrodes visible on the fluoroscopic image onto a reconstructed cortical surface by leveraging numerous common landmarks to translate, rotate, and scale coregistered computed tomography (CT) and magnetic resonance imaging (MRI) reconstructed surfaces in order to recreate the coordinate framework in which the fluoroscopic image was acquired, while accounting for parallax distortion. Validation of this approach demonstrated high precision with an average total Euclidian distance between three independent reviewers of 1.65 ± 0.68 mm across 8 patients and 82 electrodes. Spatial accuracy was confirmed by correspondence between recorded neural activity over sensorimotor cortex during hand movement. This semi-automated interface reliably estimates the location of temporarily implanted subdural ECoG electrodes visible on intraoperative fluoroscopy to a cortical surface.

Introduction

Subdural electrocorticography (ECoG) electrodes are useful clinical tools for functional mapping and seizure monitoring that can also provide detailed temporal and spatial information valuable for cognitive neuroscience research. Recent studies have employed the temporary implantation of subdural ECoG electrodes during deep brain stimulation (DBS) electrode implantation surgeries in order to simultaneously record cortical ECoG and subcortical single unit and local field potential (LFP) activity in the intraoperative setting. Initial findings using this technique suggest that patients with movement disorders, including Parkinson's disease (PD) (de Hemptinne et al., 2013, 2015; Crowell et al., 2012; Whitmer et al., 2012) and essential tremor (ET) (Air et al., 2012), have abnormal oscillatory activity recorded within the structures in the sensorimotor network. However, the lack of a reliable method for localizing the ECoG electrodes on the cortical surface in the absence of intraoperative computed tomography (CT) scanning is a limitation for the expansion of this important research opportunity. The accurate localization of these electrodes is essential for relating the recorded ECoG signals to the anatomical structures responsible for generating them.

Effective methods for the localization of subdural ECoG electrodes have been developed for clinical and research use in patients with medically refractory epilepsy. One common method uses post-operative CT to visualize implanted electrode locations that are then coregistered to their corresponding locations in pre-operative magnetic resonance imaging (MRI) space (Azarion et al., 2014; Hermes et al., 2010; Tao et al., 2009; Ken et al., 2007; Wang et al., 2013). Three-dimensional stereotactic coordinates for each electrode can then be determined on an individual reconstructed MRI. Other methods verify the electrode locations visually on the exposed brain surface with either surgical photographs or a neuro-navigational system and additionally leverages known electrode spacing to calculate the locations of non-exposed electrodes (Dalal et al., 2008; Yang et al., 2012). However, since the subdural

* Corresponding author at: Department of Neurological Surgery, University of Pittsburgh Medical Center, 200 Lothrop St., Suite B400, Pittsburgh, PA 15213, USA. Fax: +1 412 864 3441.
E-mail address: richardsonrm@upmc.edu (R.M. Richardson).
[1] These authors contributed equally to this study.

http://dx.doi.org/10.1016/j.neuroimage.2015.10.076
1053-8119/

ECoG electrodes used during DBS surgeries are only implanted temporarily and are not visible within the cranial opening, intraoperative imaging represents the only opportunity to visualize the implanted subdural electrodes. Upper extremity somatosensory evoked potential phase reversal mapping can also be used to functionally localize ECoG electrodes to the upper extremity representation of the somatosensory cortex in the post-central gyrus, but cannot localize electrodes to non-somatosensory areas of cortex. Of the options for intraoperative imaging, fluoroscopy is most often used during DBS surgeries to verify the final DBS lead position in relation to the stereotactic arc center, since intraoperative CT is not readily available in many DBS programs.

Determining the three-dimensional locations of subdural electrodes from a two-dimensional fluoroscopy image, however, is problematic due to a lack of depth information in the dimension orthogonal to the image orientation. It is possible to regain this dimension by overlaying and aligning the 2-D fluoroscopic image and corresponding 3-D anatomy to recreate the coordinate framework under which the fluoroscopic image was acquired. Many previous cortical electrode localization methods performed this coregistration by assuming that the fluoroscopic image was acquired at a perfectly lateral view (Rowland et al., 2014; Miller et al., 2007b). This assumption may imprecisely fixe rotation along all coordinate axes, limiting the ability to accurately localize cortical electrodes to a particular gyrus. One method that does account for rotation in two of the three coordinate axes utilizes post-operative fluoroscopic images in multiple orientations (Miller et al., 2010), although typically this is cumbersome in the intraoperative setting. These methods also either rely on manual placement of the reconstructed MRI within the inner skull contour (Rowland et al., 2014) or approximate alignment using the anterior–posterior commissure (AC-PC) and inioglabellar line (Miller et al., 2007b, 2010), which can introduce error to the resulting electrode locations. All previous methods additionally do not account for the distortion introduced by the parallax effect implicit in fluoroscopic images, which unrealistically magnifies objects closer to the X-ray source.

We developed a semi-automated method to localize subdural electrodes on a three-dimensional reconstructed brain using intraoperative fluoroscopy obtained during DBS electrode implantation. This method aligns coregistered pre-operative CT and post-operative MRI surfaces with an intraoperative fluoroscopic image in a manner that recreates the coordinate framework of the fluoroscopic image and simulates the parallax distortion to provide accurate and reliable electrode location estimations on the cortical surface. The reproducibility of this method was validated using multiple independent reviewers, and the accuracy of these estimations were confirmed using observed functional cortical activity.

Materials and methods

Patients

Eight patients undergoing DBS electrode implantation for the treatment of movement disorders were included in this study (7 male, 1 female, 64.4 ± 1.9 years, mean ± SE). Patient diagnoses included PD ($n = 5$) and ET ($n = 3$). DBS electrode targets were either the subthalamic nucleus (STN; $n = 4$) or the internal globus pallidus (GPi; $n = 1$) for patients with PD, and the ventral intermediate (Vim) nucleus of the thalamus ($n = 3$) for patients with ET. Six patients underwent bilateral implantation, and two patients underwent unilateral implantation.

Patients additionally had standard subdural ECoG electrodes implanted to record cortical activity for research purposes and provided informed consent for this research, which was approved by the University of Pittsburgh Institutional Review Board (#13110420). Subdural ECoG electrodes were either six or eight linear contact strips of 4 mm-diameter platinum-iridium contacts with a 2.3 mm-diameter exposed contact area and 1 cm center-to-center electrode spacing (AdTech, Racine, WI, USA). In one patient, a higher density electrode array (28 contacts, 2 mm diameter, 4 mm spacing; AdTech, Racine, WI, USA) was implanted along with a standard 8-contact electrode. Six patients had the subdural ECoG electrodes implanted on the right hemisphere, and two patients were implanted on the left. In all 8 patients, a total of 9 electrode strips over 8 hemispheres and 82 contacts were used in this analysis.

Electrode placement

Subdural ECoG electrodes were placed through the burr hole after opening the dura, but before guide tube insertion. The electrodes were aimed posteriorly to direct the distal end of the strip electrode over sensorimotor cortex, often in close approximation to the hand knob, as viewed on a cortical reconstruction in the surgical planning software (BrainLab). In one patient, an additional strip electrode was directed frontally towards the dorsolateral prefrontal cortex. Following guide tube insertion, fibrin glue was used to temporarily seal the burr hole. Once the DBS electrode was implanted, a lateral fluoroscopy image was acquired to confirm correct placement of the DBS electrode in the vertical (z-axis) and anterior–posterior (y-axis) axes. The fluoroscopic image captured the locations of the implanted subdural ECoG electrodes and at least two pin tips of the stereotactic frame. Upon confirming the placement of the DBS electrode, the subdural ECoG electrode was removed, and the DBS electrode was locked into place. Following the procedure, a post-operative MRI was obtained for additional confirmation of DBS electrode position.

Imaging data acquisition

Standard, clinically indicated imaging for DBS surgeries was used and included (1) a pre-operative stereotactic CT obtained after placement of the Leksell frame, (2) an intraoperative lateral fluoroscopic image (512 × 512 pixels, General Electric, OEC 9900), and (3) a post-operative MRI (1.5 T, Siemens Allegra). Pre-operative stereotactic CT images were acquired in contiguous axial slices with 1.5 mm thickness (General Electric, 9800). Both the pre-operative CT and intraoperative fluoroscopy were acquired with the stereotactic frame in place. MRI scans were high-resolution T1-weighted volumetric fast spoiled gradient echo (FSPGR) images (slice thickness = 1.5 mm, repetition time = 33.33 ms, echo time = 6 ms, flip angle = 35°), our standard post-operative protocol.

Image processing

All raw images were converted from the DICOM format of the scanner to NIfTI (Neuroimaging Informatics Technology Initiative) formatting and resliced with the Freesurfer image analysis suite (Dale et al., 1999). After conversion, the pre-operative CT was coregistered to the post-operative MRI using the normalized mutual information approach and then resliced in the Statistical Parameter Mapping (SPM) package (SPM12, http://www.fil.ion.ucl.ac.uk/). The accuracy of the registration was then visually verified for each patient.

Using a custom graphical user interface (Supplementary Fig. 1) within MATLAB software (The MathWorks Inc., Natick, MA, USA), DBS electrode tract locations on the post-operative MRI were visualized slice by slice as a localized reduction in signal intensity (Fig. 1A). The tracts were marked along their entire length on every other axial slice (2 mm spacing). The developed interface allows users to visualize NIfTI images in either the coronal, sagittal, or axial sections and selects desired landmarks. Using this interface, the tips of the four pins on the stereotactic frame that secure the frame to the patient's head were marked on the pre-operative CT slice images (Fig. 1B). A high-resolution reconstructed three-dimensional cortical surface model was created for each patient from post-operative MRI images using the Freesurfer suite (Dale et al., 1999). This surface was imported into MATLAB with the Freesurfer toolbox as a triangulated rendering for

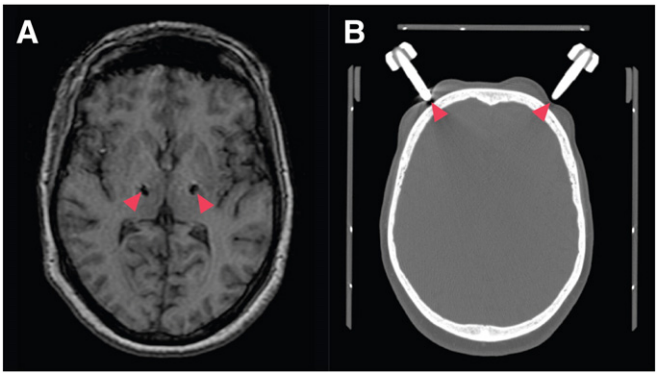

Fig. 1. Registration Landmark Localization. Localization of DBS electrode tracts on post-operative MRI (A) and stereotactic frame pins on pre-operative CT (B). These landmarks assist with registration to the intraoperative fluoroscopic image. Red arrows designate electrode locations and pin tips.

three-dimensional visualization and manipulation (Fig. 2B). A rendering of the cortical surface without any sulcal deflections or cortical hull was then calculated through Gaussian smoothing of the outer gray matter surface (Hermes et al., 2010). The coregistered and resliced CT images were imported into the Osirix software (Rosset et al., 2004) and rendered into a three-dimensional surface. Intensity threshold and smoothing parameters were adjusted to only display the skull and stereotactic frame. This surface was subsequently exported as a Wavefront object to be visualized in MATLAB as a tessellated surface (Fig. 2A).

Alignment of CT and MRI with fluoroscopic image

Coregistered cortex, cortical hull, and skull surfaces were imported into a custom graphical user interface in MATLAB along with the marked DBS electrode path(s) and stereotactic frame pin locations (Fig. 2C). Points defining each DBS electrode path were connected to form a continuous line, and the four pin tip locations were displayed as crosses for ease of visualization. The two-dimensional fluoroscopic image (Fig. 2D) was then placed in the background directly behind the surfaces (Fig. 2E). Using the camera toolbox in MATLAB, the skull surface was translated in the lateral plane and scaled to match the skull contour visible in the fluoroscopic image (Fig. 2F). The parallax effect of x-ray imaging was accounted for using the perspective projection setting in the MATLAB camera toolbox, which renders images with foreshortening relative to the distance from source to target. This source distance parameter was initially set to half of the distance between the emitter and detector, assuming the patient's head is roughly positioned at the midpoint of the C-arm. Subsequently, the source distance, translation, and rotation of the CT and MRI surfaces were adjusted in all three coordinate axes to optimize the alignment of landmarks, which included the inner and outer skull contour, DBS electrode path(s), and pin tips, to match the visible landmarks on the fluoroscopic image (Fig. 3A). To assist with alignment, the transparency of overlaid cortical and skull surfaces and the visibility of marked landmarks were adjusted. Alignment was performed with fluoroscopic images that had unilateral or bilateral DBS electrode implantation, 2–4 visible stereotactic frame pins, and partially obscured skull outlines anteriorly or posteriorly.

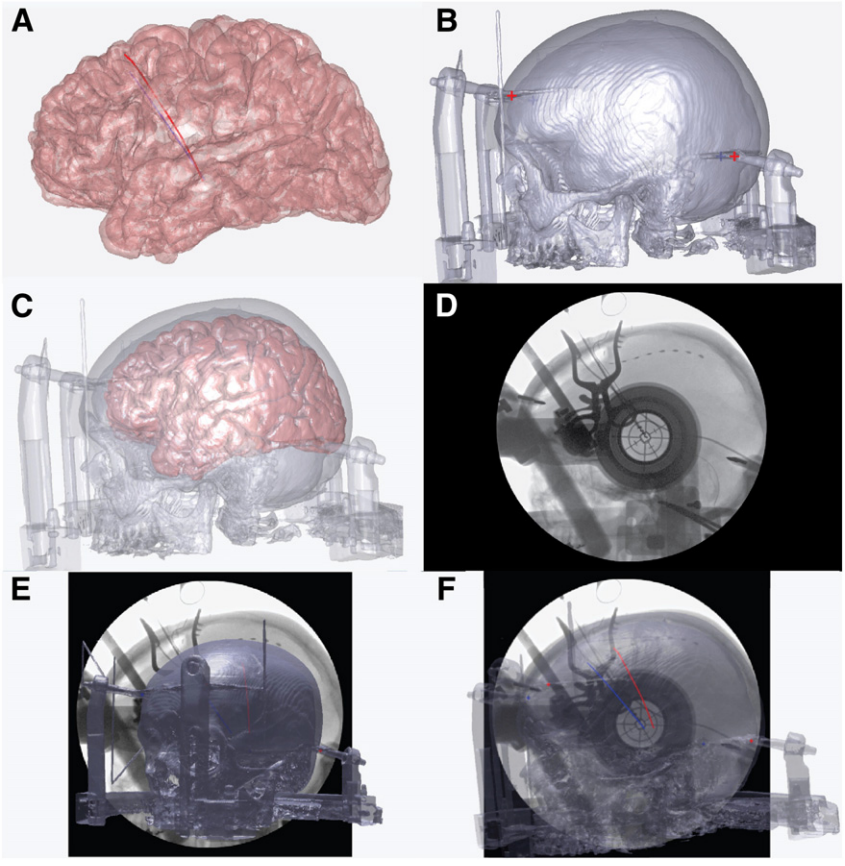

Fig. 2. Fluoroscopic image registration. (A) Reconstructed 3-D cortical surface from the post-operative MRI with DBS electrode tracts are marked as red (left) and blue (right) paths. (B) Reconstructed 3-D skull surface with attached stereotactic frame calculated from a pre-operative CT. Stereotactic frame pin tips are labeled as red (left) and blue (right) crosses to assist with registration. (C) 3-D CT and MRI surfaces coregistered using normalized mutual information coregistration. (D) Clinical intraoperative fluoroscopic image with visible stereotactic frame pins, DBS electrode tracts, skull contour, and subdural ECoG electrodes. (E) Coregistered CT and MRI (not visible) surfaces overlaid in front of the fluoroscopic image in preparation for alignment. (F) CT and MRI (not visible) surfaces after being aligned laterally and scaled to match the general outline of fluoroscopic image.

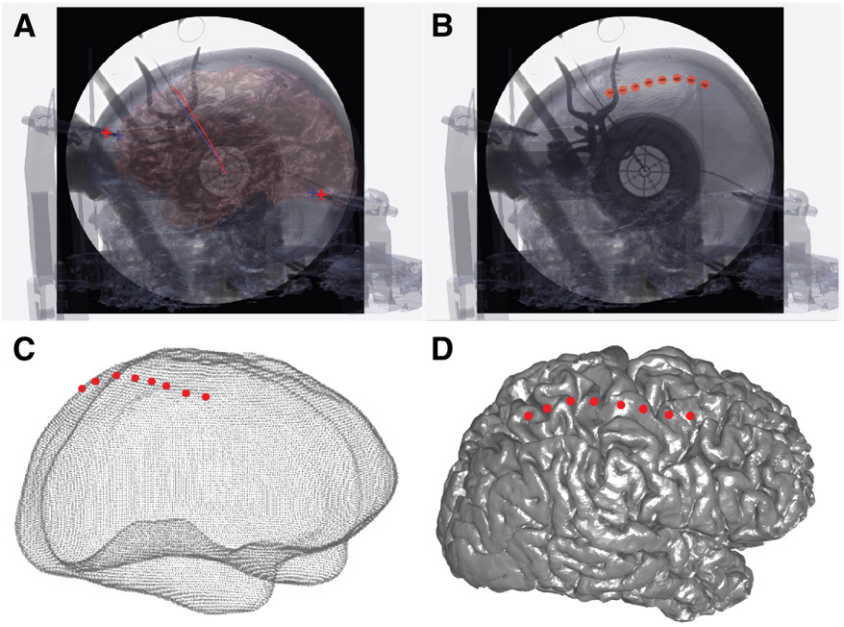

Fig. 3. Electrode localization on cortex. (A) Coregistered CT and MRI surfaces with fluoroscopic image from translational and rotational manipulations of the CT and MRI surfaces to align the marked landmarks of the DBS electrode paths and stereotactic frame pins. (B) Electrode positions marked on the fluoroscopic image. (C) Intersection points of the line created orthogonal to the electrode positions with the smoothed cortical hull. (D) Electrode locations projected and visualized on a reconstructed cortical surface.

Localization of subdural electrodes

Once the MRI and CT surfaces were registered to the fluoroscopic image, the subdural ECoG electrodes were localized to the MRI surface from the fluoroscopic image. Electrode positions on the fluoroscopic image were manually indicated by the user (Fig. 3B), whereupon a line corresponding to the user's line of sight to the electrode location was drawn through the 3-D brain coordinate space. The 3-D electrode contact location was registered to the intersection point of this line with the cortical hull of the designated hemisphere (Fig. 3C). The cortical hull was used instead of the cortical surface because it more accurately approximates how strip electrodes lie on the cortical surface and additionally minimizes errors caused by intersections that occur within deep cortical sulci. Electrode positions were then visualized on the reconstructed cortical surface (Fig. 3D).

Validation

Utility of this method relies upon precise and accurate determination of the three-dimensional coordinates of the implanted subdural ECoG electrodes on the cortical surface. Since alignment of the MRI and CT with the fluoroscopic image offers a potential source of variability between users, three independent reviewers used this method to localize electrodes, and average inter-rater variation per electrode from the mean electrode location was computed for each coordinate axis and as a total Euclidean distance. Reviewers were trained lab personnel with imaging experience, who were given an introductory tutorial about the technique, and who were blinded to each other's results.

Localization accuracy was evaluated by comparing the observation of established movement-related oscillatory changes to the anatomical electrode locations. All patients held a grip force transducer in each hand and performed an externally cued hand squeeze task during the surgical procedure. During the task, patients were instructed to provide a strong contralateral hand squeeze, a motor response expected to produce a typical cortical activation in the gamma frequency range.

Activation weights in the high frequency band (70–110 Hz) were calculated from the recordings of trials with correct responses only, by comparing spectral power during movement (1 s beginning at movement onset) and baseline (1 second prior to instructional cue) epochs on a trial-by-trial basis, as previously described (Miller et al., 2007a). Electrodes with significant ($p < 0.01$) high frequency activation (HFA) determined by a one-tailed *t*-test of the activation weights were labeled as HFA-responsive. The locations of those contacts were compared to the cortical anatomical regions defined by the Freesurfer atlas. One patient additionally underwent somatosensory evoked potential phase reversal during the procedure, and the location of the central sulcus defined by phase reversal was compared to the electrode placement (Cedzich et al., 1996).

Results

This technique localized cortical ECoG electrodes temporarily implanted during DBS surgery using routine clinical imaging. We assessed the degree to which independent reviewers could localize cortical electrode contacts to a specific location. In total, each reviewer localized 82 electrode contacts from 9 electrode strips across 8 patients. Average distance from reviewer mean location for all electrodes was 1.25 ± 0.73 mm (mean ± SD) in the medial–lateral direction (*x*-axis), 0.68 ± 0.39 mm in the anterior–posterior direction (*y*-axis), 0.62 ± 0.29 mm in the superior–inferior direction (*z*-axis), and 1.65 ± 0.68 mm total Euclidian distance. Histograms depicting both the deviations for each electrode in the *x*, *y*, *z* direction (A) and the magnitude of the total deviation (B) are shown in Fig. 4. Electrodes were localized on both the frontal and parietal cortices using only lateral fluoroscopic images. These results suggest that the localization is highly reproducible among different users.

To verify the accuracy of the localization, we examined cortical activity recorded during an externally cued hand squeeze task for high frequency activation during movement onset. Individual electrodes were classified as HFA-responsive when they exhibited significant activation during a movement epoch compared to a baseline epoch. HFA activation weights for all trials from all patients, bipolar electrode pairs and task epochs, as well as a pivot table for categorical indexing of data are available as *Data in Brief* (Randazzo et al., accompanying submission). The locations of HFA-responsive (red; $n = 23$) and non-responsive (blue; $n = 59$) electrodes were subsequently transformed and projected onto a standardized brain surface from the Montreal Neurological

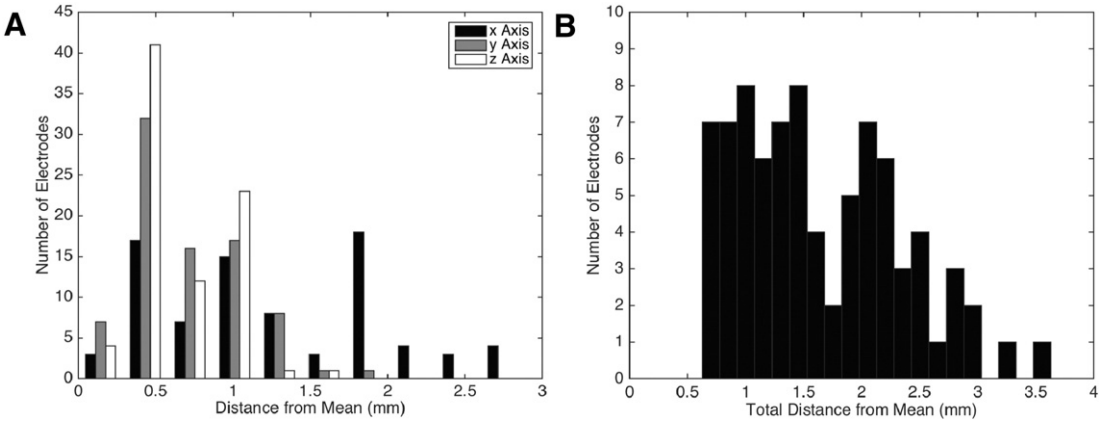

Fig. 4. Inter-rater reliability calculations. Histogram depicting the mean difference per electrode from the mean location of the reviewers in the medial–lateral direction (*x*-axis), anterior–posterior (*y*-axis), and superior–inferior (*z*-axis) directions (A) and total distance from the mean location (B).

Institute (MNI; Fig. 5A) (Saad and Reynolds, 2012). HFA-responsive electrodes were exclusively clustered on the pre- and post-central gyri as defined by the Freesurfer brain atlas. Accordingly, most non-responsive electrodes ($n = 51$) were localized to either cortical areas not known to exhibit high frequency activity during movement, or appeared to be located directly over a sulcus. Somatosensory evoked phase reversal for one subject with a high-density 28-contact strip electrode indicated the central sulcus to be between electrode pairs that the localization method also placed over the post-central gyrus, a cortical region that additionally exhibited HFA during movement (Fig. 5B).

Discussion

Recording cortical activity with subdural electrodes during DBS surgery offers a unique opportunity to gain valuable insight into the electrophysiology of movement disorders and other conditions treated with DBS. Initial electrocorticography (ECoG) studies involving patients with Parkinson's disease and essential tremor have demonstrated the utility of this technique with findings that may improve DBS therapy by supporting the development of adaptive, closed-loop DBS devices (de Hemptinne et al., 2015). This evidence builds upon numerous non-invasive neuroimaging studies using electroencephalography (EEG) (Weiss et al., 2015) and magnetoencephalography (MEG) (Heinrichs-Graham et al., 2013; Cao et al., 2015; Airaksinen et al., 2011; Olde Dubbelink et al., 2013) that investigated the underlying neurophysiology of these disorders. These non-invasive modalities, however, lack the high signal-to-noise ratio (SNR) that ECoG affords. In addition, ECoG has improved spatial resolution as compared to EEG and is able to be used in the intraoperative setting, unlike MEG.

Prior ECoG studies have been limited to studying cortical activity from a broadly identified areas within the sensorimotor cortex due to the lack of an accurate and robust method for localizing temporarily implanted subdural electrodes without intraoperative CT (Air et al., 2012; Whitmer et al., 2012; Crowell et al., 2012; de Hemptinne et al., 2013, 2015). Many methods for localizing chronic subdural electrodes exist (Azarion et al., 2014; Hermes et al., 2010; Sebastiano et al., 2006; Wang et al., 2013; Yang et al., 2012); however, most rely on post-operative imaging to visualize the electrodes in situ. Since cortical electrodes implanted during DBS surgeries are removed prior to closure, intraoperative imaging must be used to locate the electrodes. Although intraoperative CT is ideal for verifying the locations of cortical electrodes, this modality is not used routinely during DBS cases at many institutions, unlike fluoroscopy which is readily available. A challenge with using a 2-D fluoroscopic image to determine the three-dimensional coordinates of an electrode on the cortical surface is extrapolating the additional dimension. Since fluoroscopic images are most commonly not acquired from a perfectly lateral perspective, extrapolation involves constraining multiple degrees of freedom in translation, rotation, and scale. Fluoroscopy also introduces an intrinsic distortion as a result of the parallax effect, which magnifies objects as a function of distance from the emitter.

This study describes a novel method for localizing cortical electrodes on a 3-D reconstructed cortical surface from a 2-D intraoperative fluoroscopic image that (1) leverages common landmarks present in clinical fluoroscopic images acquired during DBS surgeries, (2) includes

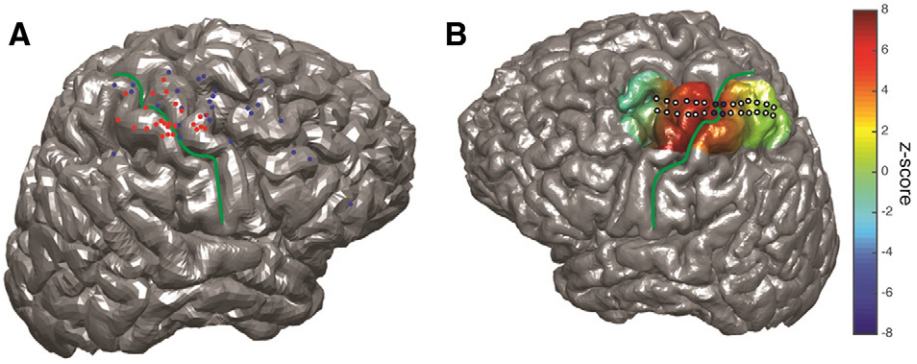

Fig. 5. Mapping of functional results. (A) Standardized cortical surface with all localized electrodes mapped. High frequency activated (HFA) electrodes during movement are shown in red ($n = 23$), and non-responsive electrodes are shown in blue ($n = 59$). HFA electrodes are clustered on the pre- and post-central gyri while most non-responsive electrodes are mapped to other areas of cortex. Non-responsive electrodes that did map to the pre- and post-central gyri are located directly over the central sulcus (green line). (B) An individual cortical surface displaying localized electrodes with HFA during movement mapped onto the cortex. HFA is expressed as the *t*-statistic of activation weights across all Go trials where the subject squeezed with the contralateral hand. Electrodes included in phase reversal results (blue circles) are seen to be bridging the central sulcus (green).

translational, rotational, and scaling manipulations in all coordinate axes, (3) accounts for the parallax distortion, and (4) does not significantly depend on the extent to which the skull contour is visible in the fluoroscopic image. The procedure involves labeling the registration landmarks including the DBS electrode paths and stereotactic frame pins, coregistration and reconstruction of the pre-operative CT and post-operative MRI, and rotational and translational alignment of the CT and MRI to the fluoroscopic image using the marked landmarks and skull contour. We found that three landmarks were sufficient to reliably constrain the degrees of freedom necessary to align the CT and MRI to the fluoroscopic image. Therefore, accurate estimations of electrode location can be performed with only a single DBS electrode, with only two visible stereotactic frame pins, or with only a portion of the skull visible. The required imaging procedures required to execute the localization are regularly performed in clinical practice, exposing the patient to no additional risk, radiation, or procedures. The localizer software package and user manual will be maintained and available for download from our laboratory website (http://www.neurosurgery.pitt.edu/research/brain-modulation-lab).

We have demonstrated that this method can be used with a variety of fluoroscopic images that include a range of visible electrodes, stereotactic frame pins, and skull contour. In terms of precision, independent reviewers were able to localize all electrodes within a three-dimensional vector distance of less than 2 mm. This inter-rater measurement error would generally not prevent reliable gyral localization. Other published methods that employ fluoroscopy have reported larger error measurements compared to intraoperative CT (x-axis: 6.0 ± 0.8 mm; y-axis: 3.3 ± 0.5 mm; z-axis: 4.0 ± 0.5 mm) (Rowland et al., 2014). The accuracy of this method was demonstrated by data showing that electrodes containing HFA in response to movement were localized to the sensorimotor cortex, while most non-responsive electrodes were localized to other regions. HFA is a known focal and somatotopically specific response observed in the contralateral sensorimotor cortex during movement onset (Crone et al., 1998, 2006; Miller et al., 2007a; Muthukumaraswamy, 2010; Pfurtscheller et al., 2003). The fact that some non-responsive electrodes were located in the peri-rolandic area likely indicates that the strip electrode missed the primary hand motor area in these cases or that a contact was directly over a prominent vein that impeded cortical recordings. Results from somatosensory evoked phase reversal, which is commonly used to localize electrode contacts to primary somatosensory cortex, exactly matched the resultant electrode placement using our localization method, in the one patient in which it was employed. These validations indicate that this method is robust enough to enable subdural ECoG electrodes to be localized in other cortical areas in which they may be placed that do not have such focal physiological biomarkers. Nonetheless, regardless of the computational approach, the technique of mapping a two-dimensional image into three-dimensional space involves some subjective measurement and is therefore the end result must be thought of as an estimation of the true electrode location.

Limitations

Potential users of this method should note that greater variability in electrode location estimations are likely to occur when only one electrode has been implanted, when the lateral fluoroscopic image is less orthogonal to the anterior–posterior course of the strip electrode, and when less of the inner and outer tables of the skull are visible on fluoroscopy. It may be possible to develop a completely automated method with an algorithm that can optimize the alignment of the CT and MRI surface landmarks with the corresponding landmarks visible in the fluoroscopic image. Optimization is necessary, since the imperfect coregistration of the CT and MRI and parallax distortion introduces an implicit error and the number of relevant landmarks exceeds the unknown rotational and translational dimensions. The alignment is further complicated due to the fact that some landmarks, such as the visible skull contour, lack reproducible discrete points that can be visualized on all three image types. Another potential improvement to the current method is the addition of an anterior–posterior (AP) fluoroscopic image obtained along with the standard lateral fluoroscopy. Although an AP image is challenging to acquire in the intraoperative setting, due to the required position of the C-arm in relation to the stereotactic frame and patient, this orientation can be useful in determining the rotation of the cortex along the sagittal plane. Another limitation of our method is the approximation of the parallax effect, which restricts the accuracy of the localization. This potential error could be further reduced with more exact measurements of the position of the patient's head between fluoroscopy emitter and detector.

Conclusion

In order to facilitate further investigation of normal and abnormal cortical activity in patients undergoing DBS surgery, we have produced a semi-automatic interface that enables users to localize subdural electrodes implanted temporarily during surgery onto a 3-D cortical surface using intraoperative fluoroscopy and routine clinical imaging. This platform enables expanded studies of the neurophysiology of disorders treated by DBS.

Supplementary data to this article can be found online at http://dx.doi.org/10.1016/j.neuroimage.2015.10.076.

Acknowledgements

We would like to thank Jim Sweat for his expert assistance in the operating room.

References

Air, Ellen L., Ryapolova-Webb, Elena, de Hemptinne, Coralie, Ostrem, Jill L., Galifianakis, Nicholas B., Larson, Paul S., Chang, Edward F., Starr, Philip A., 2012. Acute effects of thalamic deep brain stimulation and thalamotomy on sensorimotor cortex local field potentials in essential tremor. Clinical Neurophysiology 123 (11). International Federation of Clinical Neurophysiology, pp. 2232–2238. http://dx.doi.org/10.1016/j.clinph.2012.04.020.

Airaksinen, Katja, Mäkelä, Jyrki P., Taulu, Samu, Ahonen, Antti, Nurminen, Jussi, Schnitzler, Alfons, Pekkonen, Eero, 2011. Effects of DBS on auditory and somatosensory processing in Parkinson's disease. Hum. Brain Mapp. 32 (7), 1091–1099. http://dx.doi.org/10.1002/hbm.21096.

Azarion, Allan A., Wu, Jue, Davis, Kathryn A., Pearce, Allison, Krish, Veena T., Wagenaar, Joost, Chen, Weixuan, et al., 2014. An open-source automated platform for three-dimensional visualization of subdural electrodes using CT-MRI coregistration. Epilepsia 1–10 http://dx.doi.org/10.1111/epi.12827 (November).

Cao, Chunyan, Li, Dianyou, Jiang, Tianxiao, Ince, Nuri Firat, Zhan, Shikun, 2015. Resting state cortical oscillations of patients with Parkinson disease and with and without subthalamic deep brain stimulation: a magnetoencephalography study. 32 (2), 109–118.

Cedzich, Cornelia, Taniguchi, Makoto, Schafer, Sonja, Schramm, Johannes, 1996. Somatosensory evoked potential phase reversal and direct motor cortex stimulation during surgery in and around the central region. Neurosurgery 38 (May), 962–970.

Crone, N.E., Miglioretti, D.L., Gordon, B., Lesser, R.P., 1998. Functional mapping of human sensorimotor cortex with electrocorticographic spectral analysis. II. Event-related synchronization in the gamma band. Brain J. Neurol. 121 (Pt 1), 2301–2315. http://dx.doi.org/10.1093/brain/121.12.2301.

Crone, Nathan E., Sinai, Alon, Korzeniewska, Anna, 2006. High-frequency gamma oscillations and human brain mapping with electrocorticography. Prog. Brain Res. 159 (06), 275–295. http://dx.doi.org/10.1016/S0079-6123(06)59019-3.

Crowell, Andrea L., Ryapolova-Webb, Elena S., Ostrem, Jill L., Galifianakis, Nicholas B., Shimamoto, Shoichi, Lim, Daniel A., Starr, Philip A., 2012. Oscillations in sensorimotor cortex in movement disorders: an electrocorticography study. Brain 135 (2), 615–630. http://dx.doi.org/10.1093/brain/awr332.

Dalal, Sarang S., Edwards, Erik, Kirsch, Heidi E., Barbaro, Nicholas M., Knight, Robert T., Nagarajan, Srikantan S., 2008. Localization of neurosurgically implanted electrodes via photograph-MRI-radiograph coregistration. J. Neurosci. Methods 174, 106–115. http://dx.doi.org/10.1016/j.jneumeth.2008.06.028.

Dale, A.M., Fischl, B., Sereno, M.I., 1999. Cortical surface-based analysis. I. Segmentation and surface reconstruction. NeuroImage http://dx.doi.org/10.1006/nimg.1998.0395.

De Hemptinne, Coralie, Ryapolova-Webb, Elena S., Air, Ellen L., Garcia, Paul A., Miller, Kai J., Ojemann, Jeffrey G., Ostrem, Jill L., Galifianakis, Nicholas B., Starr, Philip A., 2013. Exaggerated phase-amplitude coupling in the primary motor cortex in Parkinson disease. Proc. Natl. Acad. Sci. U. S. A. 110 (12), 4780–4785. http://dx.doi.org/10.1073/pnas.1214546110.

De Hemptinne, Coralie, Swann, Nicole C., Ostrem, Jill L., Ryapolova-Webb, Elena S., San Luciano, Marta, Galifianakis, Nicholas B., Starr, Philip A., 2015. Therapeutic deep brain stimulation reduces cortical phase-amplitude coupling in Parkinson's disease. Nat. Neurosci. http://dx.doi.org/10.1038/nn.3997 (no. April).

Heinrichs-Graham, Elizabeth, Wilson, Tony W., Santamaria, Pamela M., Heithoff, Sheila K., Torres-Russotto, Diego, Hutter-Saunders, Jessica A.L., Estes, Katherine A., Meza, Jane L., Mosley, R.L., Gendelman, Howard E., 2013. Neuromagnetic evidence of abnormal movement-related beta desynchronization in Parkinson's disease. Cereb. Cortex 1–10 http://dx.doi.org/10.1093/cercor/bht121 (no. October).

Hermes, Dora, Miller, Kai J., Noordmans, Herke Jan, Vansteensel, Mariska J., Ramsey, Nick F., 2010. Automated electrocorticographic electrode localization on individually rendered brain surfaces. J. Neurosci. Methods 185 (2), 293–298. http://dx.doi.org/10.1016/j.jneumeth.2009.10.005.

Ken, Soléakhéna, Di Gennaro, Giancarlo, Giulietti, Giovanni, Sebastiano, Fabio, De Carli, Diego, Garreffa, Girolamo, Colonnese, Claudio, Passariello, Roberto, Lotterie, Jean-Albert, Maraviglia, Bruno, 2007. Quantitative evaluation for brain CT/MRI coregistration based on maximization of mutual information in patients with focal epilepsy investigated with subdural electrodes. Magn. Reson. Imaging 25 (6), 883–888. http://dx.doi.org/10.1016/j.mri.2007.02.003.

Miller, Kai J., Leuthardt, Eric C., Schalk, Gerwin, Rao, Rajesh P.N., Anderson, Nicholas R., Moran, Daniel W., Miller, John W., Ojemann, Jeffrey G., 2007a. Spectral changes in cortical surface potentials during motor movement. J. Neurosci. Off. J. Soc. Neurosci. 27 (9), 2424–2432. http://dx.doi.org/10.1523/JNEUROSCI.3886-06.2007.

Miller, Kai J., Makeig, Scott, Hebb, Adam O., Rao, Rajesh P.N., den Nijs, Marcel, Ojemann, Jeffrey G., 2007b. Cortical electrode localization from x-rays and simple mapping for electrocorticographic research: the 'location on cortex' (LOC) package for MATLAB. J. Neurosci. Methods 162 (1-2), 303–308. http://dx.doi.org/10.1016/j.jneumeth.2007.01.019.

Miller, Kai J., Hebb, Adam O., Hermes, Dora, den Nijs, Marcel, Ojemann, Jeffrey G., Rao, Rajesh N.P., 2010. Brain Surface Electrode Co-Registration Using MRI and X-Ray. Conference Proceedings: … Annual International Conference of the IEEE Engineering in Medicine and Biology Society. IEEE Engineering in Medicine and Biology Society. Conference 2010 (January), pp. 6015–6018 http://dx.doi.org/10.1109/IEMBS.2010.5627597.

Muthukumaraswamy, Suresh D., 2010. Functional properties of human primary motor cortex gamma oscillations. J. Neurophysiol. 104 (September), 2873–2885. http://dx.doi.org/10.1152/jn.00607.2010.

Olde Dubbelink, Kim T.E., Hillebrand, Arjan, Stoffers, Diederick, Berend Deijen, Jan, Twisk, Jos W.R., Stam, Cornelis J., Berendse, Henk W., 2013. Disrupted brain network topology in Parkinson's disease: a longitudinal magnetoencephalography study. Brain 137, 197–207. http://dx.doi.org/10.1093/brain/awt316.

Pfurtscheller, G., Graimann, B., Huggins, J.E., Levine, S.P., Schuh, L.A., 2003. Spatiotemporal patterns of beta desynchronization and gamma synchronization in corticographic data during self-paced movement. Clin. Neurophysiol. 114 (7), 1226–1236. http://dx.doi.org/10.1016/S1388-2457(03)00067-1.

Rosset, Antoine, Spadola, Luca, Ratib, Osman, 2004. OsiriX: an open-source software for navigating in multidimensional DICOM images. J. Digit. Imaging 17 (3), 205–216. http://dx.doi.org/10.1007/s10278-004-1014-6.

Rowland, Nathan C., Miller, Kai J., Starr, Philip A., 2014. Three-dimensional accuracy of ECOG strip electrode localization using coregistration of preoperative MRI and intraoperative fluoroscopy. Stereotact. Funct. Neurosurg. 92 (1), 8–16. http://dx.doi.org/10.1159/000350027.

Saad, Ziad S., Reynolds, Richard C., 2012. Suma. NeuroImage 62, 768–773. http://dx.doi.org/10.1016/j.neuroimage.2011.09.016.

Sebastiano, F., Di Gennaro, G., Esposito, V., Picardi, A., Morace, R., Sparano, A., Mascia, A., Colonnese, C., Cantore, G., Quarato, P.P., 2006. A Rapid and Reliable Procedure to Localize Subdural Electrodes in Presurgical Evaluation of Patients with Drug-Resistant Focal Epilepsy. Clin. Neurophysiol. 117 (2), 341–347. http://dx.doi.org/10.1016/j.clinph.2005.10.005.

Tao, James X., Hawes-Ebersole, Susan, Baldwin, Maria, Shah, Sona, Erickson, Robert K., Ebersole, John S., 2009. The Accuracy and Reliability of 3D CT/MRI Co-Registration in Planning Epilepsy Surgery. Clinical Neurophysiology: Official Journal of the International Federation of Clinical Neurophysiology 120 (4). International Federation of Clinical Neurophysiology, pp. 748–753. http://dx.doi.org/10.1016/j.clinph.2009.02.002.

Wang, Po T., King, Christine E., Shaw, Susan J., Millett, David E., Liu, Charles Y., Chui, Luis A., Nenadic, Zoran, Do, An H., 2013. A Co-Registration Approach for Electrocorticogram Electrode Localization Using Post-Implantation MRI and CT of the Head. 2013 6th International IEEE/EMBS Conference on Neural Engineering (NER). IEEE, pp. 525–528 http://dx.doi.org/10.1109/NER.2013.6695987 (November).

Weiss, D., Klotz, R., Govindan, R.B., Scholten, M., Naros, G., Ramos-Murguialday, A., Bunjes, F., et al., 2015. Subthalamic stimulation modulates cortical motor network activity and synchronization in Parkinson's disease. Brain 1–15 http://dx.doi.org/10.1093/brain/awu380.

Whitmer, Diane, de Solages, Camille, Hill, Bruce, Yu, Hong, Henderson, Jaimie M., Bronte-Stewart, Helen, 2012. High frequency deep brain stimulation attenuates subthalamic and cortical rhythms in Parkinson's disease. Front. Hum. Neurosci. 6 (June), 1–18. http://dx.doi.org/10.3389/fnhum.2012.00155.

Yang, Andrew I., Wang, Xiuyuan, Doyle, Werner K., Halgren, Eric, Carlson, Chad, Belcher, Thomas L., Cash, Sydney S., Devinsky, Orrin, Thesen, Thomas, 2012. Localization of dense intracranial electrode arrays using magnetic resonance imaging. NeuroImage 63 (1). Elsevier Inc., pp. 157–165. http://dx.doi.org/10.1016/j.neuroimage.2012.06.039.